

Another Look at the Separation of P- and S-Waves

Jun-Wei Huang*
University of Toronto, Toronto, ON, Canada
jhuang@physics.utoronto.ca

and

Bernd Milkereit
University of Toronto, Toronto, ON, Canada

Inspired by full waveform 3-D elastic modeling, a new approach for P- and S-wave separation is developed based on the divergence and curl operations on vectorial wave fields in the depth-time domain. In VSP geometry, the required neighboring wave field for spatial derivatives is approximated by the wave field generated by shifted sources and acquired by the same receivers. We test this method on 2C-2D and 3C-3D synthetic VSP data with and without random noise. This method shows its effectiveness in separating synthetic P and S data with low signal-to-noise ratios generated in heterogeneous media with strong contrasts. In the numerical simulations of walkaway VSPs, it generally works better in attenuating the P energy in the S energy component than in attenuating the S energy in the P energy component. The restriction to the source location shifting is determined by the primary wavelength and the heterogeneity of the medium.

Introduction

Elastic seismic data consist of compressional (P) and shear (S) waves representing different rock properties. In heterogeneous reservoirs with strong contrasts, offset VSP surveys with varying angles of incidence may generate strong converted waves that contaminate the source generated P- and S-wave arrivals. Separation of P- and S-waves and recovering their full amplitude therefore are important for proper processing and interpretation of the data.

P-S wave separation was initiated by Dankbaar (1985) and was applied to both 3-component surface data (Dankbaar, 1985) and VSP data (Dankbaar, 1987). This method relied on the calculation of filter coefficients in the f - k domain using estimated velocities. The f - k transformation may cause smearing of energy due to data aliasing. The critical concern associated with the methods developed in the f - k domain is to reduce the artifacts due to the edge of the filters. The median filter, a nonlinear filter without f - k response, can separate source generated P- and S-waves if an appropriate length is chosen. But it has difficulty in dealing with PS/SP conversions. Polarization analysis (DiSiena et al, 1984) was also developed to extract P- or S-wave energy based on the assumption that the polarization directions of P- and S-waves are orthogonal (Lei, 2005). Here we propose a different way of separating P- and S-waves based on 2C-2D and 3C-3D synthetic data.

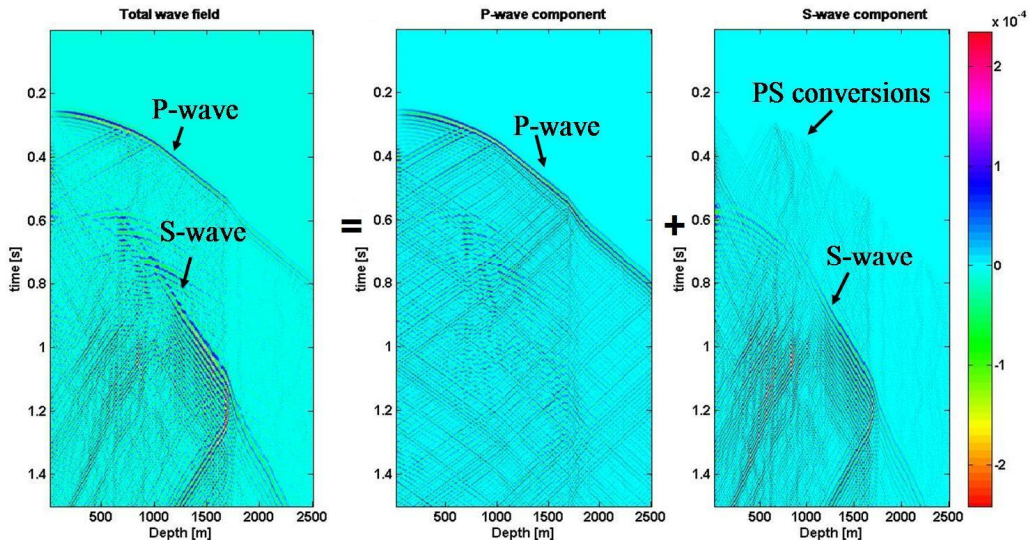


Figure 1. Synthetic VSP data with acquisition geometry of only two source points. The total wave field (horizontal component) can be decomposed into a P-wave component and an S-wave component by using divergence and curl operations.

Background

Lamé's theorem (Aki & Richards, 1980) states that the displacement $\mathbf{u}(x,y,z,t)$ can be written as

$$\mathbf{u} = \nabla\phi + \nabla \times \boldsymbol{\psi} \quad (1.1)$$

where $\nabla\phi$ and $\nabla \times \boldsymbol{\psi}$ are called the P-wave and S-wave components of \mathbf{u} , respectively. By definition the divergence ($\nabla\phi$) and curl ($\nabla \times \boldsymbol{\psi}$) operators can be expressed as

$$\nabla\phi = \frac{\partial\phi}{\partial x} \mathbf{i} + \frac{\partial\phi}{\partial y} \mathbf{j} + \frac{\partial\phi}{\partial z} \mathbf{k}, \text{ and } \nabla \times \boldsymbol{\psi} = \left(\frac{\partial\psi_z}{\partial y} - \frac{\partial\psi_y}{\partial z} \right) \mathbf{i} + \left(\frac{\partial\psi_x}{\partial z} - \frac{\partial\psi_z}{\partial x} \right) \mathbf{j} + \left(\frac{\partial\psi_y}{\partial x} - \frac{\partial\psi_x}{\partial y} \right) \mathbf{k}$$

where \mathbf{i} , \mathbf{j} , \mathbf{k} are the unit vectors in x , y , and z direction, respectively.

Therefore the P-wave component and S-wave component can be extracted by vector processing:

$$\nabla \cdot \mathbf{u} = \nabla^2\phi \quad (1.2)$$

$$\nabla \times \mathbf{u} = \nabla \times (\nabla \times \boldsymbol{\psi}) \quad (1.3)$$

Although most seismograms record velocity or acceleration instead of displacement, equation (1.2) and (1.3) are still valid for temporal derivatives of \mathbf{u} . Explicitly, we write $\mathbf{v}(x,y,z,t) = \dot{\mathbf{u}}(x,y,z,t)$ and thus P-wave energy and S-wave energy can be calculated in the following way:

$$\bar{E}_p = \left(\frac{\partial v_x}{\partial x} + \frac{\partial v_y}{\partial y} + \frac{\partial v_z}{\partial z} \right) \sqrt{\pi} \quad (1.4)$$

$$\bar{E}_s = \text{sign}(\varepsilon_s) \sqrt{\varepsilon_s} \quad (1.5)$$

$$\text{where } \varepsilon_s = \mu \left[\left(\frac{\partial v_y}{\partial z} - \frac{\partial v_z}{\partial y} \right) \left| \frac{\partial v_y}{\partial z} - \frac{\partial v_z}{\partial y} \right| + \left(\frac{\partial v_z}{\partial x} - \frac{\partial v_x}{\partial z} \right) \left| \frac{\partial v_z}{\partial x} - \frac{\partial v_x}{\partial z} \right| + \left(\frac{\partial v_x}{\partial y} - \frac{\partial v_y}{\partial x} \right) \left| \frac{\partial v_x}{\partial y} - \frac{\partial v_y}{\partial x} \right| \right]$$

Here \bar{E}_p and \bar{E}_s are the P- and S-component energy respectively, v_i denotes particle velocity in the i direction, $\pi = \lambda + 2\mu$ and μ are the compressional modulus and shear modulus of the media, respectively (Dougherty & Stephen, 1988).

In numerical simulations the full wave field is available for divergence and curl operations; the P-wave component and S-wave component can be separated completely (figure 1). In practice however, seismograms are only part of the full wave field and thus lack some information for equation (1.4) and (1.5). For example, in borehole seismic data, $x=x_0$ and $y=y_0$, and only z is the independent variable, i.e., $\mathbf{v} = \mathbf{v}(x_0, y_0, z, t; \mathbf{s})$ with t for time and $\mathbf{s} = (s_x, s_y)$ for the vector of source position. In order to apply divergence and curl operations, the vectorial wave field in the vicinity of the receivers is required. Therefore we propose the approximation in equation (1.6). The required wave fields for spatial derivatives are approximated by the wave fields generated by shifted source locations (figure 2).

$$\begin{aligned} \frac{\partial v_i}{\partial x} &= \frac{v_i(x_0 + \Delta x, y_0, z, t; \mathbf{s}) - v_i(x_0 - \Delta x, y_0, z, t; \mathbf{s})}{2\Delta x} \\ &\approx \frac{v_i(x_0, y_0, z, t; s_x - \Delta x) - v_i(x_0, y_0, z, t; s_x + \Delta x)}{2\Delta x} \\ \frac{\partial v_i}{\partial y} &= \frac{v_i(x_0, y_0 + \Delta y, z, t; \mathbf{s}) - v_i(x_0, y_0 - \Delta y, z, t; \mathbf{s})}{2\Delta y} \\ &\approx \frac{v_i(x_0, y_0, z, t; s_y - \Delta y) - v_i(x_0, y_0, z, t; s_y + \Delta y)}{2\Delta y} \\ \frac{\partial v_i}{\partial z} &= \frac{v_i(x_0, y_0, z + \Delta z, t; \mathbf{s}) - v_i(x_0, y_0, z - \Delta z, t; \mathbf{s})}{2\Delta z} \end{aligned} \quad (1.6)$$

where $i=x, y, z$ is the i^{th} component of vectorial wave field, Δx and Δy are the horizontal shifting, and Δz is the depth sample interval. Thus the wave field generated by a horizontally shifted source is equivalent to the horizontal shifting of receivers in the borehole and equations (1.4), (1.5) can be calculated.

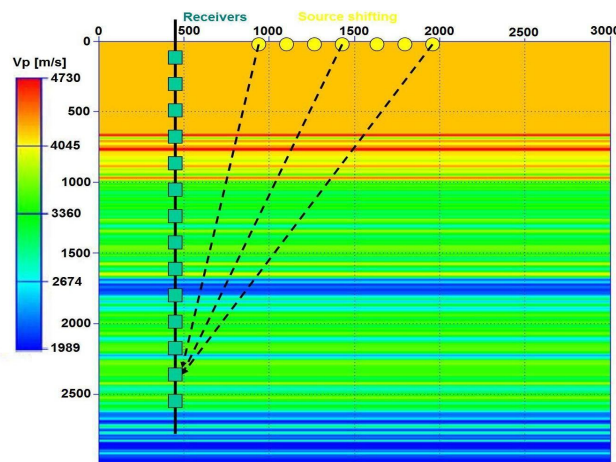


Figure 2. The schematic graph illustrates that the wave field in the vicinity of the borehole is estimated by the wave field generated by the laterally shifting source. This figure also shows the acquisition geometry of 2C-2D offset VSP from a layered model modified from Mallik gas hydrate research borehole logs (Milkereit et al., 2005). The source horizontal shifting is $1400 \text{ m} \pm 200 \text{ m}$.

Synthetic Results from Layered Media

The layered model (figure 2) is constructed based on the well logs from borehole Mallik 2L-38 (Milkereit et al., 2005). The offset VSP data are generated by sources between horizontal coordinates 1200 m and 1600 m with 10 m intervals. Due to the 2nd-order approximation of spatial derivatives, either P-wave energy or S-wave energy cannot be attenuated completely (figure 3). The remnant S-wave energy in P-wave component and the remnant P-wave energy in S-wave component (figure 3) are attenuated up to -20dB compared to the ideally separated S-wave and P-wave components (figure 1), respectively. The attenuation results can be improved by using higher order spatial derivatives, i.e., more than two source locations. In order to quantify the effectiveness of separation, the P-wave energy and the S-wave energy distribution areas are defined in the $f-k$ domain. The ratios of P- or S-wave amplitude to the summation of the whole P- or S-wave amplitude are used to assess the effectiveness. When the source lateral shifting reaches 60 m, i.e., $0.6\lambda_p$ or $1.2\lambda_s$, the ratio arrives at a plateau. This phenomenon results from the increasing of the undesired remnant energy in the wanted energy component, and indicates an optimum source shifting distance may exist. The energy smearing due to the $f-k$ transform can influence the accuracy of this assessment criterion. In the presence of random noise, similar results can be achieved but it is more difficult to quantify the effectiveness of separation due to the noise contamination in the $f-k$ domain. The approach can be easily applied to 3-D layered models but more computation resources are required.

Conclusions and Outlook

This paper presents a new strategy to separate P- and S-waves in 3C-3D VSP data using vector processing technique: divergence and curl. Numerical simulations demonstrate the effectiveness in attenuating undesired energy. This method can be easily applied to 3C-3D VSP and surface data from individual Vibroseis sweeps of a source array before summation. It can also be used in seismic data processing such as stacking. Further investigation on the effectiveness and acquisition geometries with over two source locations are needed. Application to real data will be tested.

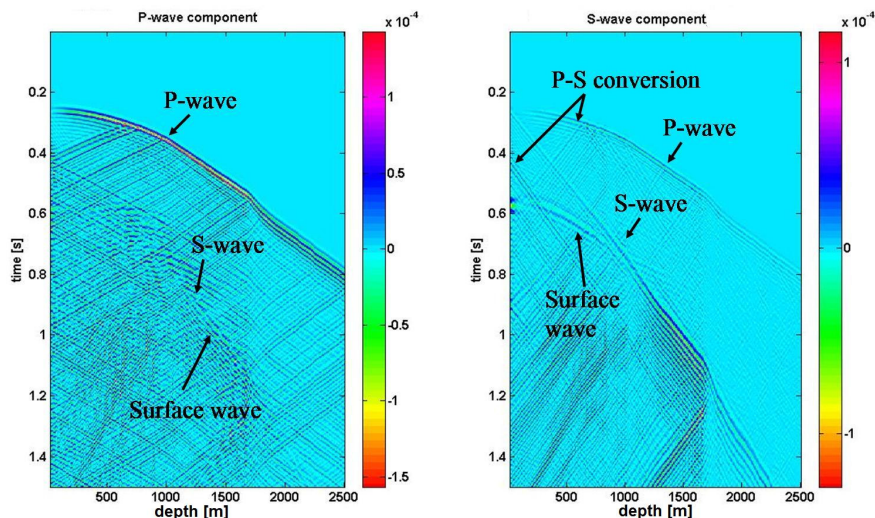


Figure 3. P- and S-wave energy components from 2C-2D synthetic VSP data with a simple two source points acquisition geometry. The remnant direct S-wave energy in P-wave component and the remnant direct P-wave energy in S-wave component are attenuated up to -20dB compared to the ideally separated S-wave and P-wave components, respectively (see figure 1).

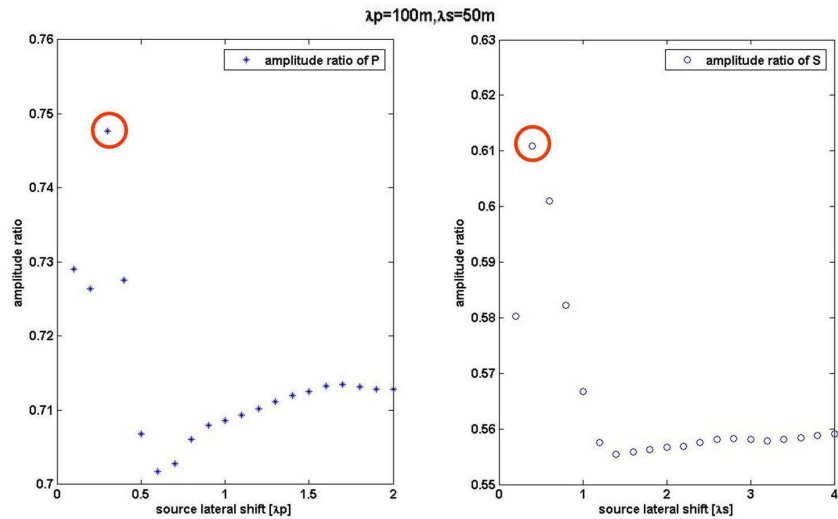


Figure 4. Ratio of P-wave (left) and S-wave (right) amplitudes. The primary wavelengths of the P-wave and S-wave are about 100 m and 50 m, respectively. When the source lateral shifting reaches 60 m ($0.6\lambda_p$ or $1.2\lambda_s$), the ratio arrives at a plateau which indicates the increase of remnant energy outside of the wanted energy region. The red circles mark the maximum amplitude ratio and the corresponding P-wave and S-wave components are shown in figure 3.

References

- Dankbaar, J.W.M. 1985, Separation of P and S waves. *Geophysical Prospecting* 33, 970-986.
- Dankbaar, J.W.M. 1987, Vertical Seismic Profiling – Separation of P- and S- waves, *Geophysical Prospecting* 35, 803-814.
- DiSiena, J.P., Gaiser, J.E., and Corrigan, D., 1984, Horizontal components and Shear Wave Analysis of Three-component VSP data, in *Vertical Seismic Profiling, Part B: Advanced Concepts* edited by M. Nafi Toksoz and Robert R. Stewart,
- Dougherty & Stephen, 1988, Seismic Energy Partitioning and Scattering in Laterally Heterogeneous Ocean Crust. *Pure and Applied Geophysics*, 128, 195 - 239.
- Milkereit, B., Adam, E., Li, Z., Qian, W., Bohlen, T., Banerjee, D., and Schmitt, D.R., 2005, Multi-offset vertical seismic profiling: an experiment to assess petrophysical-scale parameters at the JAPEX/JNOC/GSC et al. Mallik 5L-38 gas hydrate production research well; in *Scientific Results from Mallik 2002 Gas Hydrate Production Research Well Program, Mackenzie Delta, Northwest Territories, Canada*, (ed.) S.R. Dallimore and T.S. Collett; Geological Survey of Canada, Bulletin 585, 13p.
- Lei, J., 2005, A method for non-orthogonal seismic polarization-vector separation, *Geophysics Journal International*, 162, 965-974.